

Experimental Research on the Impact of Anchor-Cable Tensions in Mooring Ship at Vung Tau Anchorage Area

Xuan Phuong Nguyen[#], Nguyen Dang Khoa Pham[#]

[#]Ho Chi Minh City University of Transport, Ho Chi Minh City, Vietnam
E-mail:phuong@ut.edu.vn

Abstract— According to the detailed planning of Southeast seaport group up with an orientation to 2030, Ba Ria - Vung Tau seaport is an international gateway (type IA), acting as an international transshipment port where commercial, industrial services are developed and facilitated in goods import and export activities. However, one of the significant obstacles to the development of the Ba Ria-Vung Tau port service industry is the lack of synchronous infrastructure of the entire port system. The leading causes of these obstacles are due to inappropriate design and investment in anchoring and lack of in-depth studies on the specific characteristics of the flow through the anchorage area. This is a big problem, because the tankers often have low freeboard, mainly affecting the flow in the mooring area. Therefore, the focus on studying the impact of the flow in the anchored area of Vung Tau on oil tankers will contribute to the maritime practice of the anchoring areas in general and in Vung Tau in particular. In this paper, the authors will focus on empirical research on an experimental model that is constructed by the uniform method to determine the anchor-cable tension of ship anchorages with different loading modes at the assumed flow rate in the anchoring areas in Vung Tau. The results obtained from experimental research and simulation by numerical methods are compared and evaluated to develop an empirical and reliable formula for anchor-cable tension with oil tankers in Vung Tau anchorage area.

Keywords—anchoring area; anchor-cable tension; Vung Tau ports; seaport system.

I. INTRODUCTION

According to the overall planning of Vietnam's seaport system and the detailed planning of the group of seaports in the Southeast region (group 5), Ba Ria - Vung Tau port (BR-VT) will be one of the 2 ports of the international gateway type IA [1]. The BR-VT port is planned to be developed to meet the requirements of receiving a growing fleet of world ships, sharing the number of goods through Ho Chi Minh City seaport [2], and gradually play a significant role as an international gateway port in the southern region. If implemented by the plan, by 2030, BR-VT seaport will handle through a cargo volume of 162-296 million tons/year, becoming the largest seaport in the entire seaport system in Vietnam [3].

It is lame to compare the current capacity scale of BR-VT seaport with the principal seaports of Southeast Asia. The main terminals of the BR-VT seaport have only been built and put into operation in the last 10 years[4]. While regional container ports such as PSA Singapore started operating in the 1970s; Tanjung Pelepas (PTP) port in Malaysia began operations in 2000 [5]; Port Kelang, Malaysia has deep-water harbors started operating in the 1970s and thrived since 1983. In 2010, PSA Singapore port handled 28.43 million TEU of container cargo, Laem Chabang handled

5.19 million TEU, and Cai Mep - Thi Vai (CM-TV) handled only about 0.5 million TEU [6].

However, at this time, shipping lines in the world's TOP 20 (according to the statistics 4.2018) such as APM-Maersk (No. 1), CMA-CGM (3rd), Hanjin Shipping (9th), has participated in joint ventures to invest in construction and operation of CM-TV regional ports such as CMIT, Gemadep Terminal Link, TCIT, My Xuan International Synthesis, and some ports have been put into operation such as CMIT, TCIT[1]. In addition, the presence of investors is the leading port operators in the world such as PSA (Singapore) in the joint venture investment and operation of SP-PSA port, Hutchison Port Holdings (Hong Kong) in a joint venture to invest in the operation of SITV port with efforts to modernize and professionalize domestic port operators, have upgraded the organization, management and operating system at CM-TV terminals equivalent to the leading ports in Southeast Asia. According to statistics, every year, on average, about 40,000 cruise ships sail through the area of Ganh Rai Bay of Vung Tau to enter and leave ports of the 5th seaport; Ganh Rai Bay averages 5,000 to 7,500 ships annually [7].

The main harbor area of the BR-VT seaport is currently the CM-TV area, which is an area with geographical location and natural conditions very favorable for port

a big problem because the tankers often have low freeboard; the effect is mainly due to the flow in the anchorage[17]. Therefore, the focus on studying the impact of the flow in the anchored area of Vung Tau on oil tankers will contribute to the maritime practice of the anchoring areas in general and in Vung Tau in particular.

Currently, in universities, research institutes of maritime science in advanced countries around the world have focused on solving a series of problems around the impact of the ocean current (flow) on the ship. For example, studies evaluating the effects of the dynamics of the flow around the ship, the image of the hull profile to the propeller of the ship, the effects of waves, wind, ...[18] However, studies on the influence of ocean currents on maneuvering ships [19], on the issue of drifting or breaking ties in anchorage are of little interest[20]. In Vietnam, many scientists and managers in the field of hydrodynamics have also developed and published several results related to the impact of ocean circulation in general on ships[21]. However, for these results to be applied in maritime scientific practice, there are many difficulties [22]. This requires a link between many scientists in different fields to solve the scientific tasks set out. In Vietnam, no formal studies have been published on this issue yet. Therefore, it is necessary to study the impact of ocean currents on the anchoring of ships in mooring areas[23]. This study can combine simulation research[24] with experimental research on the model to assess the accuracy of the methods to determine the tension of anchor-cable. On that basis, recommendations were made to limit errors due to the effects of ocean currents which were rare and not yet widely published[21].

The construction of the problem model is closest to the real world so that we can study the hypotheses of different situations, from which there are warnings to minimize marine accidents in anchoring areas in general and Vung Tau in particular, especially with the fleet of tankers due to the freeboard, the flow is less noticeable. In this paper, the authors have developed an empirical research plan from which to set up an experimental research process; Design and manufacture of equipment for experimental research. The empirical research results are analyzed to evaluate the feasibility and reliability of the experimental model.

II. MATERIALS AND METHODS

A. Experimental model

The authors propose a system for experimental research to determine the tension of anchors, as shown in Figure 2.

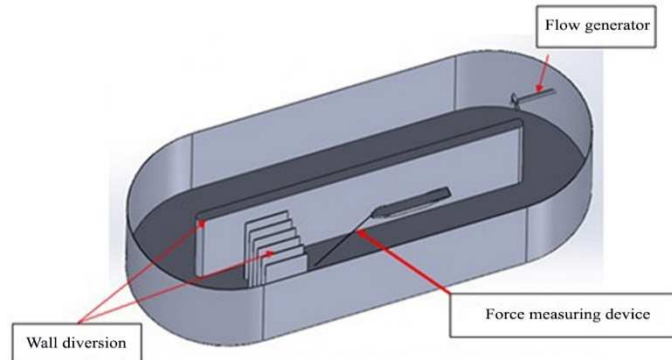


Fig. 2 Diagram of the principle of the experimental research problem

Flow generator: Axial vane pump can be used to create flow in a circulation system as shown. Pump flow and channel cross-section will give us the velocity of flow. Thus, it is possible to adjust the pump flow or adjust the channel cross-section to change the desired flow velocity. The deflector is placed in the middle of the housing, made of thick steel, to guide the flow into the propeller smoothly and direct the exit flow, to ensure water flow through the propeller of the propeller for the smooth, stable and efficient operation of the propeller. Figure 3 describes the dimensions and shape of the guide flow in the system's water tank.

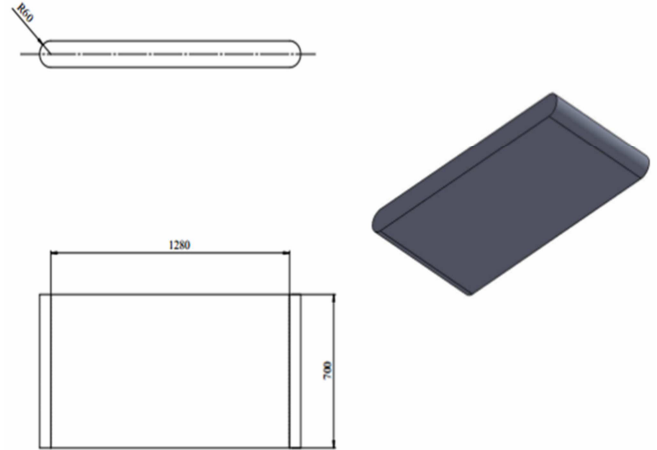


Fig. 3 Design and manufacture of diversion part for recirculating water tanks

Circulating flow system: In addition to combining with a circulating flow pump, we can use the channel cross-section to change the desired flow rate; Anchor-cable and tension measuring device: The anchor-cables are created to satisfy the same type as the anchor-cables of the real problem[25]. On the mooring cables, a tension gauge of the cable will be installed; Hull: Designed similarly to Aulac Jupiter vessel of Au Lac Joint Stock Company, the geometric congruence ratio is $k = 100$, with different draft lines corresponding to 3 load modes: full load, half load, and no load.

The water tank is made of thick steel, the total capacity of nearly 2.7 m^3 of water, including the shell and diversion. The shell of the specific design dimensions is depicted in Figure 4, and the shape of the tank shell is in Figure 5.

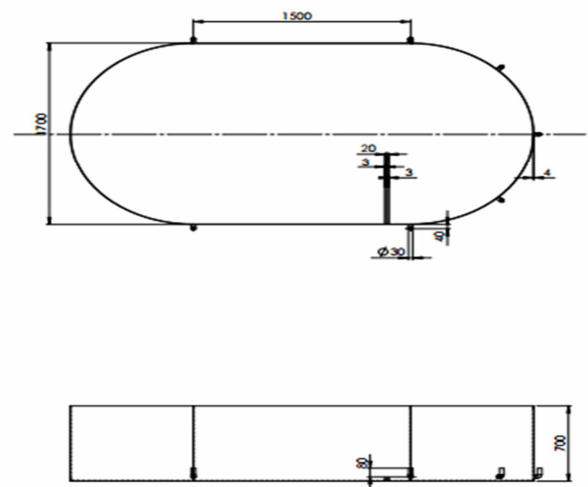


Fig. 4 Design dimensions and fabrication of water tank shell

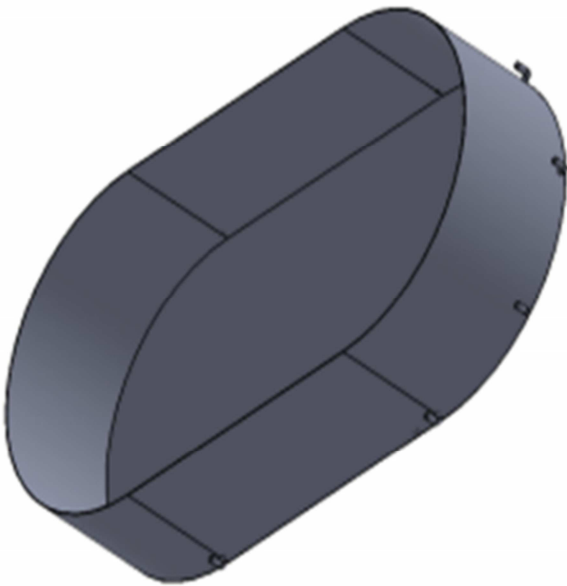


Fig. 5 Design and fabrication of circulating water tank shell

Frame lifting system and moving (Figure 6): This is a support for the entire system and can move quickly to ensure maneuverability in the process of exploitation and repair later, designed to ensure technical standards[26].The entire lifting frame is mounted by a load-bearing (three-wheel) wheel system, and the front is mounted with a single wheel, the rear is fitted with two wheels and the guide system, axle and bearing systems are calculated and selected to ensure technical standards [27].

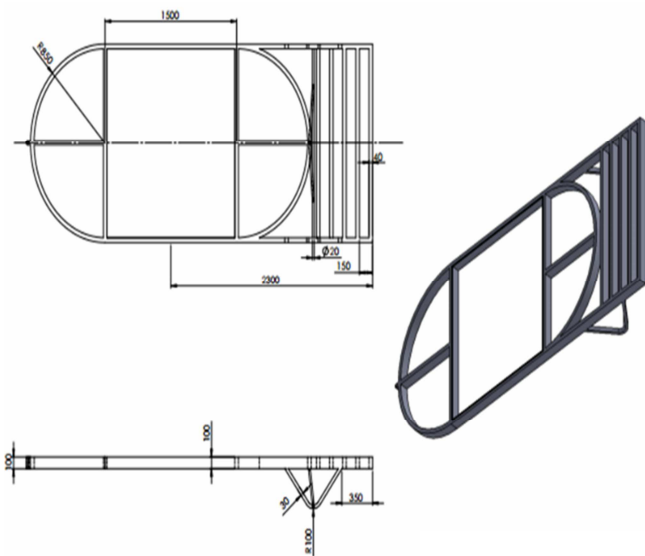


Fig. 6 Design and manufacture of test system lift frame

B. Aulac Jupiter hull model

Designed similarly to Aulac Jupiter ship of Au Lac Joint Stock Company, the geometric congruence ratio is $k = 100$; some pictures show the process of building a ship model (Figure 7): Images of ship models built using NAPA software for 3D printing to support the next step of covering composite materials. After covering with composite materials, the surface will be smoothed, painted, and drawn to show the draft for experimental research.



Fig. 7 Image of ship model after fabrication

C. Instrumentation

1) Force measuring device:

TABLE II
FORCE MEASUREMENT EQUIPMENT PARAMETERS

Manufacturer	SAUTER
Model	FK 100
Measuring range (max)	100 N (10kg)
The resolution	0,05 N
Accuracy	0,5 % of [Max]
Frequency of measurement	1000 Hz
Reading function	Real-time or Peak Hold
Unit	N, lb, kg, oz
Dimensions WxDxH	195x84x35 mm
Accessories	adapter (tow hook, pointed, flat, 90m extension link)

2) Device for measuring flow rate: To control the accuracy of the flow rate in the channel, we use a hand-held velocity meter, as shown as photo s of equipment after installation (Figure 8).

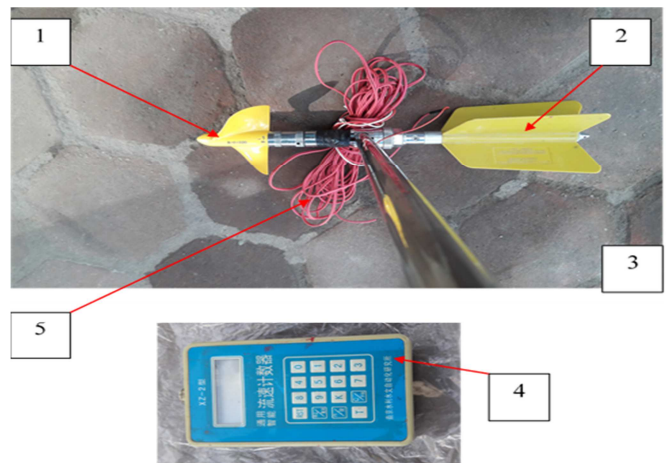


Fig. 8 Image of XZ-2 flow velocity meter

- 1- axial turbine: is the unit to convert the energy of the flow to be measured into the number of revolutions of the turbine;
- 2 - flow direction: helps the flow meter always parallel with the flow when dropping down the flow to be measured;
- 3-handle: helps bring the instrument down to the flow in different depths;
- 4-devices display the measured value;
- 5-conductor: transmits measurement signal to display device.

D. Experimental process

An experimental process on the established model should be tested with the condition: Creating 5 different flow rates and 3 different drafts. Thus, there are a total of 15 pairs of the input value-added output value is the anchor tension value, combined with a comparison with the simulated calculation by CFD, we show details in the following Table 3:

TABLE III
SUMMARY OF EXPERIMENTAL RESEARCH PLANS

Flow velocity (knot)	Anchor-cable tension force R (N) (on calculation model)					
	No-load		Half-load		Full-load	
	CFD	Experiment	CFD	Experiment	CFD	Experiment
2.0						
2.5						
3.0						
3.5						
4.0						
Flow velocity (knot)	Anchor-cable tension force R (N) (on real ships, with uniform coefficient $k = 100$)					
	2.0					
	2.5					
	3.0					
	3.5					
4.0						

Table 3 shows the amount of work that needs to be carried out in experimental research. Thus, when experimental results are available, we will revise the calculation model using numerical methods. It is entirely possible to expand the problem to study for different flow rates. In particular, we can assume the instability of the flow and wind velocity acting on the ship to calculate the corresponding anchor-cable tension [24].

The experimental process should be conducted according to the following steps: (i) Prepare (electrical system, water pump; make sure the equipment is assembled correctly). (ii) Control draft parameters (by placing the load on the hull to adjust the draft as desired) and force measuring device. Figure 9 shows the location of the anchor-cable tension gauge, making sure the measuring device is not stuck or friction with other devices, the measurement value will be updated continuously during the survey. The draft is controlled by a line on the hull with 3 values corresponding to 3 modes: full load, half load, and no load. (iii) Commissioning and adjusting flow parameters. This is an important step to accurately control the flow rate according to the experimental research plan set out. Based on the operating principle diagram of the pump used. As shown in Figure 10, the control of the flow rate through the channel and surrounding anchored hull is calculated by the flow of pump Q and the cross-section of the channel. Therefore, to adjust the flow velocity to the desired values (5 values according to the empirical research scheme), we have two ways to adjust: (a) *Method 1*: Change the flow of the pump by adjusting the pump directly, this results in the pump having this feature; (b) *Method 2*: Use a pump with a flow mode, but we change the section of the channel section containing the hull and anchor. (iv) Record the data of anchor-cable tension at the survey site. (v) Change the working point (go back to step ii to iv). (vi) Finish (shutdown, clean and dry the system).

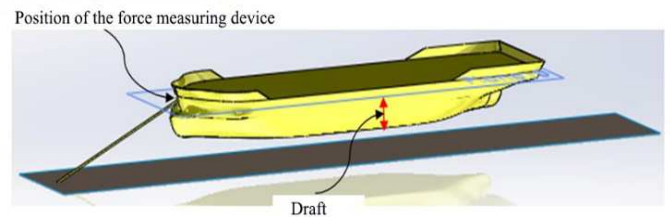


Fig. 9 Draft control and force measuring device

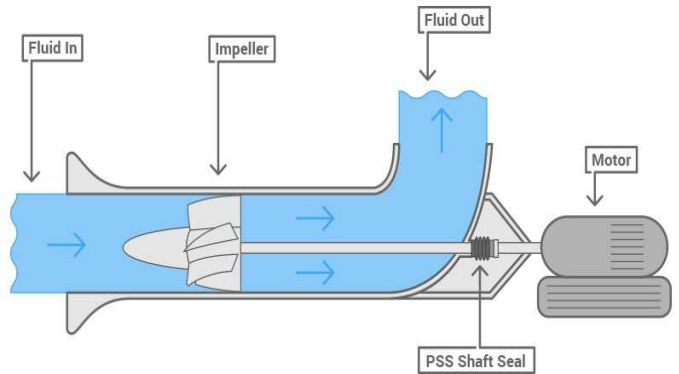


Fig. 10 Schematic of a channel connected to a pump

III. RESULTS AND DISCUSSION

The results calculated by CFD give us the value of the force acting on the hull caused by the flow R_x (Table 4). To compare with experimental research results, we first need to convert the force acting on this hull into the tension of the anchor-cable. The layout of anchor-cable and analysis of the force acting on the anchor-cable is arranged as follows Figure 10.

TABLE IV
SUMMARY OF OPTIONS AND RESULTS OF CFD CALCULATION

Flow velocity (knot)	Anchor-cable tension force R (N) (on calculation model)					
	No-load		Half-load		Full-load	
	CFD	Experiment	CFD	Experiment	CFD	Experiment
2.0	0.513		1.037		1.800	
2.5	0.626		1.258		2.190	
3.0	0.737		1.469		2.578	
3.5	0.847		1.740		3.000	
4.0	0.954		1.874		3.320	
Flow velocity (knot)	Anchor-cable tension force R (N) (on real ships, with uniform coefficient k = 100)					
	2.0	0.513*10 ⁶		1.037*10 ⁶		1.800*10 ⁶
	2.5	0.626*10 ⁶		1.258*10 ⁶		2.190*10 ⁶
	3.0	0.737*10 ⁶		1.469*10 ⁶		2.578*10 ⁶
	3.5	0.847*10 ⁶		1.740*10 ⁶		3.000*10 ⁶
	4.0	0.954*10 ⁶		1.874*10 ⁶		3.320*10 ⁶

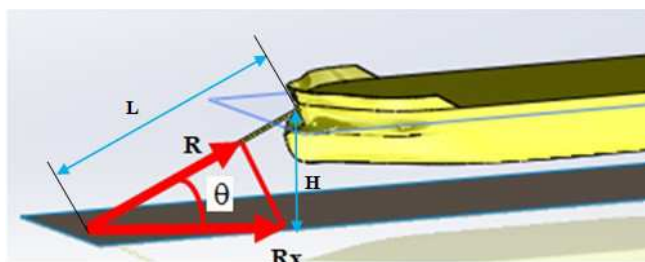


Fig. 11 The layout of anchor-cable and analysis of force acting on anchor-cable

Through Figure 11, we determine the slope angle θ of the anchor-cable concerning the bottom plane in the critical case (straight anchor-cable):

$$\sin\theta = H/L \quad (1)$$

where:

H- Height from hole to bottom in anchoring area;

L- Length of anchor-cable.

Based on the analysis of the force acting on the anchors (Figure 10), we calculate the tension of the anchor-cable R:

$$R = R_x \cdot \cos\theta \quad (2)$$

For the similarity study, according to Aulac Jupiter vessel of Au Lac Joint Stock Company, other parameters refer to Vung Tau mooring area. Specific figures see the following Figure 12:

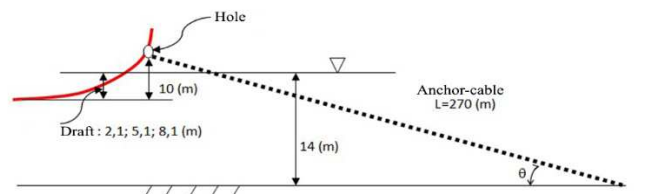


Fig. 12 Diagram of mooring cable for Aulac Jupiter at Vung Tau mooring area

Through Figure 11, depending on 3 draft states, we will have 3 cases where the angle of anchor rope is different, namely: No-load: a draft of 2.1 m: $\cos\theta=0.9967$; Half load: draft is 5.1 m: $\cos\theta=0.9975$; No-load: a draft of 2.1 m: $\cos\theta=0.9982$. We calculate the tension of anchor rope as shown in Table 5. Summing up the experimental research results and comparing them with the CFD calculation in Table 6.

TABLE V
SUMMING UP THE RESULTS OF THE CALCULATION OF ANCHOR TENSION BY CFD

Flow velocity (knot)	On the model Aulac Jupiter					
	No-load		Half-load		Full-load	
	CFD		CFD		CFD	
	R _x (N)	R(N)	R _x (N)	R(N)	R _x (N)	R(N)
2.0	0.513	0.5113	1.037	1.0344	1.800	1.7960
2.5	0.626	0.6239	1.258	1.2548	2.190	2.1860
3.0	0.737	0.7345	1.469	1.4653	2.578	2.5730
3.5	0.847	0.8442	1.740	1.7350	3.000	2.9940
4.0	0.954	0.9508	1.874	1.8693	3.320	3.3140

Research results show that the tension force of anchor-cable obtained by CFD is always higher than the experiment. Moreover, they all reflect the fact that the tension force of anchor-cable depends significantly on the flow velocity, when the flow velocity increases, the tension force of the anchor-cable increases sharply. According to simulation studies, the tension force of anchor-cable increases almost linearly according to the flow velocity, an increase of about 115% compared to the first state. Meanwhile, in experimental studies, the data shows that the anchor-cable tension force depends on many external factors, so the increasing tendency of anchor-cable tension force does not seem to be linear with the flow velocity.

The load modes have played a massive role in the anchor-cable tension of the ship; the anchor-cable tension force increases about 3.5 times when the load increases to the full-load level in both simulation and experimental tests on the model of Aulac Jupiter. In other cases, when the flow velocity is rising, the tendency of anchor-cable tension increases with rising load. The increase in resistance when increasing the load is more significant than the increase in the flow velocity. This shows that the danger status will be more evident when the ship is anchored with loads. The higher the load, the greater the tension in the anchor-cable, which means the higher the risk when the ship is at mooring.

TABLE VI
SUMMING UP THE RESULTS OF CALCULATING THE CABLE TENSION BY CFD
AND EXPERIMENT

Flow velocity (knot)	Anchor-cable tension force R (N) (on the model of Aulac Jupiter)					
	No-load		Haft-load		Full-load	
	CFD	Experiment	CFD	Experiment	CFD	Experiment
2.0	0.5113	0.5012	1.0344	0.9158	1.7960	1.6234
2.5	0.6239	0.5342	1.2548	1.1265	2.1860	2.0376
3.0	0.7345	0.6548	1.4653	1.3258	2.5730	2.3879
3.5	0.8442	0.7321	1.7350	1.6145	2.9940	2.7458
4.0	0.9508	0.8678	1.8693	1.7478	3.3140	3.1247
Flow velocity (knot)	Anchor-cable tension force R (N) (on real ships, with uniform coefficient k = 100)					
2.0	0.5113 *10 ⁶	0.5012 *10 ⁶	1.0344 *10 ⁶	0.915 8*10 ⁶	1.7960 *10 ⁶	1.6230*1 0 ⁶
2.5	0.6239 *10 ⁶	0.5342 *10 ⁶	1.2548 *10 ⁶	1.126 5*10 ⁶	2.1860 *10 ⁶	2.0370*1 0 ⁶
3.0	0.7345 *10 ⁶	0.6548 *10 ⁶	1.4653 *10 ⁶	1.325 8*10 ⁶	2.5730 *10 ⁶	2.3870*1 0 ⁶
3.5	0.8442 *10 ⁶	0.7321 *10 ⁶	1.7350 *10 ⁶	1.614 5*10 ⁶	2.9940 *10 ⁶	2.7450*1 0 ⁶
4.0	0.9508 *10 ⁶	0.8678 *10 ⁶	1.8693 *10 ⁶	1.747 8*10 ⁶	3.3140 *10 ⁶	3.1240*1 0 ⁶

From the results obtained in Table 6, a comparative evaluation of the two alternatives with different load cases is essential.

- **No-load:** With the results in Table 6, the average deviation between CFD calculation and experimental research is 11.1%, the most significant deviation at the flow rate of 2.5 m/s is 16.8%.
- **Half-load:** With the results in Table 6, the average deviation between CFD calculation and experimental research is 9.8%, the most significant deviation at the flow rate of 2.0 m / s is 13%.
- **Full-load:** With the results in Table 6, the average deviation between CFD calculation and experimental research is 8.2%, the most significant deviation at the flow rate of 2.0 m / s is 10.6%.

IV. CONCLUSION

The paper has established a simulation process and experimental research to determine the tension of mooring lines and mooring lines for ships at any mooring area. Application with a specific tanker, Aulac Jupiter, and reference data at Vung Tau mooring area (anchoring characteristics, flow information ...) to formulate the tension formula of mooring rope (R_{ln}) and mooring line (R_{db}). The impact of the ocean current on the ship when it is anchored at different loads (full load, half load, and no-load), calculating the anchor-cable tension with different intensity and direction of flow.

The effects of ocean currents on the ship when loading goods at different loads (full load, half load, and no-load), calculation of anchor-cable tension with different intensities and directions of flow. Develop and implement an experimental research process to demonstrate some simulated calculation results. The experimental object was a specific M/T Aulac Jupiter tanker, flow parameters and geometric dimensions based on data at Vung Tau mooring area.

Based on the results of simulation calculations and experimental research with the object of Aulac Jupiter tanker, give the tension formula of anchor-cable (R_{ln}) and mooring rope (R_{db}), applied in Vung Tau area. Thus, comparing with the critical tension of anchor-cable and mooring rope used will give a danger warning for users. After calculating and simulating the problem to determine the cable tension and applied to Aulac Jupiter tanker and other parameters refer to at Vung Tau mooring area such as flow rate range, channel depth. In this study, the authors teamed up with the same modeling design to conduct empirical research that gave the calculation results at 15 working points corresponding to 3 different drafts. Therefore, with 3 different load modes, we will have 3 functions that determine the relevant tension. Each load mode we have 5 working points (5 different flow rates). In practice of maneuvering ships with a flow rate other than 5 points, what is the tension of anchor-cable? With current mathematical tools, it is possible to apply interpolation to construct an approximate function that passes through 5 known points, putting out the tension on the remaining points is only a number change.

REFERENCES

- [1] W. Y. Yap, "Container trade and shipping connectivity of Vietnam: Implications of Comprehensive and Progressive Agreement for Trans-Pacific Partnership and 21st Century Maritime Silk Road," *International Journal of Shipping and Transport Logistics*. 2019.
- [2] X. P. Nguyen, "The bus transportation issue and people satisfaction with public transport in Ho Chi Minh city," *J. Mech. Eng. Res. Dev.*, 2019.
- [3] C. Kontgis, A. Schneider, J. Fox, S. Saksena, J. H. Spencer, and M. Castrence, "Monitoring peri-urbanization in the greater Ho Chi Minh City metropolitan area," *Appl. Geogr.*, 2014.
- [4] H. T. Pham and H. Lee, "Developing a Green Route Model for Dry Port Selection in Vietnam," *Asian J. Shipp. Logist.*, vol. 35, no. 2, pp. 96–107, 2019.
- [5] T. M. H. Le, H. R. Choi, and L. A. M. Alfarc, "An exploratory study on policy of the public-private partnership to develop seaport in Vietnam," *Int. J. Appl. Bus. Econ. Res.*, 2017.
- [6] F. Rusgiyanto, A. Sjafruddin, R. B. Frazila, Suprayogi, and J. T. Burhani, "Inland container depots effect for import container terminal performance at Koja container terminal, Jakarta based on optimization–simulation model," in *AIP Conference Proceedings*, 2018, vol. 1977, no. 1, p. 20038.
- [7] P. Rosa-Santos, F. Taveira-Pinto, and F. Veloso-Gomes, "Experimental evaluation of the tension mooring effect on the response of moored ships," *Coast. Eng.*, 2014.
- [8] T. H. Hoang, A. T. Hoang, and V. S. Vladimirovich, "Power generation characteristics of a thermoelectric modules-based power generator assisted by fishbone-shaped fins: Part I-effects of hot inlet gas parameters," *Energy Sources, Part A Recover. Util. Environ. Eff.*, 2019.
- [9] A. T. Hoang, Q. V. Tran, A. R. M. S. Al-Tawaha, V. V. Pham, and X. P. Nguyen, "Comparative analysis on performance and emission characteristics of an in-Vietnam popular 4-stroke motorcycle engine running on biogasoline and mineral gasoline," *Renew. Energy Focus*, vol. 28, pp. 47–55, 2019.
- [10] T. T. Nguyen, "An Investigation of the Vietnamese Shipping Industry and Policy Recommendations for Profound Participation

- into ASEAN Integration,” *Asian J. Shipp. Logist.*, vol. 32, no. 2, pp. 81–88, 2016.
- [11] X. T. Nguyen, Y. Park, and J. Park, “A Quantitative Marine Traffic Safety Assessment of the Vung Tau Waterway,” *J. Navig. Port Res.*, 2012.
- [12] V. T. H. Thu, T. Tabata, K. Hiramatsu, T. A. Ngoc, and M. Harada, “Effects of sea level rise and sea dike construction on the downstream end of the Saigon River Basin (Can Gio Bay),” *Japan Agric. Res. Q.*, 2018.
- [13] A. T. Hoang and V. V. Pham, “A review on fuels used for marine diesel engines,” *J. Mech. Eng. Res. Dev.*, vol. 41, no. 4, pp. 22–32, 2018.
- [14] J. K. Hsieh, Y. C. Hsieh, H. C. Chiu, and Y. C. Feng, “Post-adoption switching behavior for online service substitutes: A perspective of the push-pull-mooring framework,” *Comput. Human Behav.*, 2012.
- [15] K. H. Lee, H. S. Han, and S. Park, “Failure analysis of naval vessel’s mooring system and suggestion of reducing mooring line tension under ocean wave excitation,” *Eng. Fail. Anal.*, 2015.
- [16] J. Davidson and J. V. Ringwood, “Mathematical modelling of mooring systems for wave energy converters - A review,” *Energies*, 2017.
- [17] J. Palm, C. Eskilsson, G. M. Paredes, and L. Bergdahl, “Coupled mooring analysis for floating wave energy converters using CFD: Formulation and validation,” *Int. J. Mar. Energy*, 2016.
- [18] E. Roszko, “Maritime territorialisation as performance of sovereignty and nationhood in the South China Sea,” *Nations Natl.*, 2015.
- [19] P. H. Hoang, A. T. Hoang, N. H. Chung, L. Q. Dien, X. P. Nguyen, and X. D. Pham, “The efficient lignocellulose-based sorbent for oil spill treatment from polyurethane and agricultural residue of Vietnam,” *Energy Sources, Part A Recover. Util. Environ. Eff.*, vol. 40, no. 3, pp. 312–319, 2018.
- [20] A. T. Hoang and V. V. Pham, “Impact of jatropha oil on engine performance, emission characteristics, deposit formation, and lubricating oil degradation,” *Combust. Sci. Technol.*, vol. 191, no. 03, pp. 504–519, 2019.
- [21] A. T. Hoang, “A report of the oil spill recovery and treatment technologies to reduce the marine environment pollution,” *Int. J. e-Navigation Marit. Econ.*, vol. 9, pp. 35–49, 2018.
- [22] X. P. Nguyen and H. N. Vu, “Corrosion of The Metal Parts of Diesel Engines In Biodiesel-Based Fuels,” *Int. J. Renew. Energy Dev.*, vol. 8, no. 2, 2019.
- [23] M. Hall and A. Goupee, “Validation of a lumped-mass mooring line model with DeepCwind semisubmersible model test data,” *Ocean Eng.*, 2015.
- [24] N. D. Khoa Pham and X. Phuong Nguyen, “Application of CFD for calculation and simulation of anchor-cable tensions in mooring ship,” *J. Mech. Eng. Res. Dev.*, 2019.
- [25] A. T. Hoang, A. T. Le, and V. V. Pham, “A core correlation of spray characteristics, deposit formation, and combustion of a high-speed diesel engine fueled with Jatropha oil and diesel fuel,” *Fuel*, vol. 244, pp. 159–175, 2019.
- [26] T. M. Hao Dong and X. Phuong Nguyen, “Exhaust Gas Recovery From Marine Diesel Engine In Order To Reduce The Toxic Emission And Save Energy: A Mini Review,” *J. Mech. Eng. Res. Dev.*, 2019.
- [27] V. Paulauskas, “Ship and Quay Wall Mooring System Capability Evaluation,” in *Transportation Research Procedia*, 2016.